Proceedings of the 10th World Congress on Civil, Structural, and Environmental Engineering (CSEE 2025)
Barcelona, Spain - April 13 - 15, 2025
Paper No. ICGRE 107
DOI: 10.11159/icgre25.107

An Experimental Study of the Parameters Affecting the Compression Index of Clay Soil

Rami Mahmoud Bakr,
Delta University for Science and Technology
Gamassa, Intenational coastal road, Egypt
ramibakr2000@yahoo.com, ramibakr2000@deltauniv.edu.eg,
https://orcid.org/0000-0003-1498-1084,

Abstract - The constant rate of strain (CRS) test is a rapid technique that effectively measures specific properties of cohesive soil, including the rate of consolidation, hydraulic conductivity, compressibility, and stress history. Its simple operation and frequent readings enable efficient definition, especially of the compression curve. However, its limitations include an inability to handle strain-rate-dependent soil behavior, initial transient conditions, and pore pressure evaluation errors. There are currently no effective techniques for interpreting CRS data. In this study, experiments were performed to evaluate the effects of different parameters on CRS results. Extensive tests were performed on two types of clay to analyze the soil behavior during strain consolidation at a constant rate. The results were used to evaluate the transient conditions and pore pressure system.

Keywords: Constant Rate of Strain (CRS), Resedimented Boston Blue Clay (RBBC), Resedimented Vicksburg Buckshot Clay (RVBC), Compression Index

1. Introduction

Compacted clays are utilized in construction as engineering barriers, especially for waste disposal repositories at shallow depths, because of their retention properties, high exchange capacity, and low permeability. Such repositories are subjected to various temperature cycles because of the climate changes that occur over their service lives, which can be greater than 10,000 years. These changes may affect the hydro-mechanical properties of the compacted clays, especially the creep and compressibility, which can degrade the long-term performance of the repository. Compression and swelling indices seem to be unaffected by temperature, although yield stress reduces with increasing temperature, according to a research on the long-term effects of temperature on compacted clays, particularly addressing creep. Time plays a role in the secondary compression, with creep strains decreasing over the course of 10 days to stabilise at a constant value. An increase in effective stress or temperature results in a higher creep coefficient (Kaddouri; Z.; Cuisinier et al., 2019).

Various emerging technologies have been developed for identifying and analyzing functional parameters to resolve various geo-environmental issues in civil engineering. Environmental computation (EC) complements conventional but unrealistic assumptions with the advantages of machine learning (ML). Improving fine-grained soils such as clay require understanding the correlation of soil properties with its behavior. Soil compressibility is an essential property that describes the reduction in soil volume under a load as pore water is drained. Accurate evaluation of the soil compressibility is pivotal for measuring the settlement of soil layers, especially fine-grained- soils owing to their low permeability. The compression index (Cc) is a commonly utilized parameter to define soil compressibility. Various empirical equations have been developed to identify Cc, which are often used together with statistical analysis. However, this approach is limited owing to the low correlation between output and input parameters (Onyelowe; K.C.; et al., 2021).

Identifying soil behavior is important for determining whether problems persist under various load conditions. The settlement and bearing capacity are critical considerations for engineering structures. At present, instances where loads on the structure exceed the bearing capacity of the foundation rarely happen. However, the settlement of the foundation may eventually exceed permissible values depending on the soil properties. Settlement can be time-dependent or immediate, depending on the soil type. Because of the high permeability of coarse-grained soils, immediate settlement is dominant. For fine-grained soils such as clay, time-dependent settlement takes place.

The main objective of this study was to find a strong correlation between Cc and these parameters (water content [w], hydraulic conductivity [k], and excess pore water pressure/total stress [Δu/σ]), which are easily measured, and to evaluate the effects of the parameters on the results of the constant strain of rate (CRS) test. The parameters need to be calibrated to guarantee consistency. The effects of the soil type, strain rate, devices, and analysis techniques on the consistency of the CRS test results were evaluated.

The rest of the paper is organized as follows. Section 2 reviews the existing literature. Section 3 explains the research methodology. Section 4 presents the results. Section 5 concludes the paper.

2. Literature Review

Settlement occurs when the stress in soil layers increases as a result of the presence of a structure. For shallow foundations, the criteria of settlement-based design are vital (Kaddouri; Z.; Cuisinier et al., 2019) and (Onyelowe; K.C.; et al., 2021). Terzaghi's one-dimensional consolidation theory may be used to determine volume change characteristics of clays for the oedometer test (Akbarimehr; D. and Aflaki; et al., 2019). The slope of the curve representing the void ratio (e) against the logarithm of the effective pressure is the compression index (Cc), a parameter quantifying the material compressibility. Furthermore, the Cc value, the principal indicator of soil compressibility, is often used for determining the settlement of soil layers (Kaddouri; Z.; Cuisinier et al., 2019), and (Mohammadzadeh S; D; et al., 2019). The parameter Cc is essential in determining the main consolidation settlement of clays [5]. A high Cc value indicates a significant settlement. Determining the Cc values using oedometer tests is time-consuming and expensive (Liu et al. 2019; Pandya et al. 2019; Alam et al. 2021; Shahriar et al. 2018). Additionally, an oedometer test is tedious because it depends on accuracy, sensitivity, and experience. Even a minor disturbance can cause an error in determining the Cc value and the settlement. Thus, calculating the Cc value could save a lot of time and experimental cost if correlations between the Cc value and readily obtained soil parameters are developed (Fikret Kurnaz; T.; et al., 2019). As a result, several studies have been conducted to reliably predict the Cc value from the already established soil parameters. Table 1 shows the proposed equations, which may include one or more variables for predicting the Cc value, defining liquid limit (LL), natural water content (n), in-situ void ratio (eo), specific gravity (Gs), and dry unit weight (γd) for various water contents and densities. Evaluating uncertain and ambiguous input parameters for any empirical estimates is necessary. Table 1 also presents some multiparameter correlations. Multiple regression-based correlations provide a more reliable assessment of the compression index (However, the evaluated variables must be completely independent of each other, and the physical significance of the mathematical process must be considered to obtain reliable correlations based on multiple linear regression (Li and White 1993; Cherubini and Giasi 2000; Giasi et al. 2003).

Table 1: Some correlations between index properties and consolidation parameters.

Correlation	Applicability	References
$C_c = 0.01w_n$	All clays	Koppula (1981)
$C_c = 0.01(w_n - 7.549)$	Clays	Rendon-Herrero (1983)
$C_c = 0.0115w_n$	Organic silt and clays	Bowles (1979)
$C_c = 0.01(w_n - 5)$	All clays	Azzouz et al. (1976)
$C_c = 0.006(LL - 9)$	All clays with LL <100 %	Azzouz et al. (1976)
$C_c = 0.008(LL - 12)$	All clays	Sridharan and Nagaraj (2000)
$C_c = 0.009(LL - 10)$	All clays	Terzaghi and Peck (1967)
$C_c = 0.063(LL - 10)$	Egyptian clay	Mahmoud and Abdrabbo (1990)
$C_c = 0.048(LL - 10)$	Brazilian clays	Bowles (1979)
$C_c = 0.007(LL - 10)$	Remoulded clays	Skempton (1944)
$C_c = 0.0046(LL - 9)$	Brazilian clays	Cozzolino (1961)
$C_c = 0.009(LL - 10)$	NC clays	Terzaghi and Peck (1967)
$C_c = 0.009(LL - 8)$	Osaka Bay clay	Tsuchida (1991)
$C_c = 0.009LL$	Tokio Bay clay	Tsuchida (1991)
$C_c = 0.008(LL - 12)$	All clays	Sridharan and Nagaraj (2000)

$C_c = 0.007(SI + 18)$	All clays	Sridharan and Nagaraj (2000)
$C_c = 0.014(PI + 3.6)$	All clays	Sridharan and Nagaraj (2000)
$C_c = PI/74$	All Clays	Wroth and Wood (1978)
$C_c = 0.29(e_0 - 0.27)$	Inorganic soils	Hough (1957)
$C_c = 0.35(e_0 - 0.5)$	Organic soils	Hough (1957)
$C_c = 0.156e_0 + 0.0107$	All clays	Bowles (1979)
$C_c = 1.15(e - e_0)$	All clays	Nishida (1956)
$C_c = 0.29(e_0 - 0.27)$	Inorganic soils	Hough (1957)
$C_c = 0.35 (e_0 - 0.5)$	Organic soils	Hough (1957)
$C_c = 0.246 + 0.43 (e_0 - 0.25)$	Motley clays: Sao Paulo, Brazil	Cozzolino (1961)
$C_c = 1.21 + 1.055 (e_0 + 1.87)$	Lowland of Santos, Brazil	Cozzolino (1961)
$C_c = 0.75(e_0 - 0.5)$	Soils with low plasticity	Sowers (1970)
$C_c = 0.208e_0 + 0.0083$	Chicago clays	Bowles (1979)
$C_c = 0.156e_0 + 0.0107$	All clays	Bowles (1979)
$C_c = 0.2343(LL/100)\ G_s$	All clays	Nagaraj and Murty (1985)
$C_c = 0.2926(LL/100)\ G_s$	All clays	Nagaraj and Murty (1985)
$C_c = 0.5\ G_s(PI/100)$	All Clays	Wroth and Wood (1978)
$C_c = 0.009w_n + 0.005LL$	All Clays	Koppula (1981)
$C_c = 0.037(e_0 + 0.003LL - 0.34)$	Clays: Greece, parts of the USA	Azzouz et al. (1976)
$C_c = -0.156 + 0.411e_0 + 0.00058LL$	All Clays	Al-Khafaji and Andersland (1992)
$C_c = 0.048(e_0 + 0.001w_n - 0.25)$	Clays: Greece, parts of the USA	Azzouz et al. (1976)
$C_c = 0.37(e_0 + 0.003LL + 0.0004w_n - 0.34)$	Clays: Greece, parts of the USA	Azzouz et al. (1976)

3. Research Methodology

The procedures and equipment utilized in this study were in accordance with the techniques and devices implemented via different research projects, including laboratory tests of cohesive soils. Tests were performed on different clayey soils to investigate the effects of the applied strain rate on different soil types. CRS tests normally utilize the Wissa constant rate of the strain device along with nonlinear and linear analysis techniques.

3.1 Materials

Resedimented Boston blue clay (RBBC) was utilized because its engineering properties have been properly established by laboratory tests in previous research, and its properties have been comprehensively modeled. Furthermore, the behavior of RBBC is representative of uncemented and natural clay deposits. Hence, its results can be generalized to different deposits with adjustments made to accommodate the conditions of particular sites. In this study, RBBC refers to marine clays sedimented in the Boston basin.

Resedimented Vicksburg buckshot clay (RVBC) was utilized as a uniform material with known and constant properties, which facilitated comparison with the RBBC samples. Natural VBC is a fat clay with high plasticity. In addition, RVBC has been selected as a reference soil for quality assurance and quality control. For RVBC, 1.4 litre of water was utilized in the batch experiments.

Resedimented Vicksburg silt (RVS) was selected owing to its use in other research on batch tests of different soil types. RVS samples are prepared similarly to RVBC samples. Two batches were developed by combining slurry with 1.2 L of water to realize a water content of 70%.

3.2. Constant Rate of Strain Test

The CRS test evaluates the consolidation of a soil specimen subjected to uniform deformation by a strain-controlled loading frame. The CRS test was established, in which the stress on the specimen and the pore water pressure at the base continually recorded (Hamilton and Crawford,1959). Several theories have been proposed to model the change in pore pressure within a specimen. The selection of the strain rate is critical for the CRS test.

3.2.1. Apparatus

A conventional fixed-ring consolidation cell with a triaxial compression machine was utilized to apply the deformation (Hamilton and Crawford, 1959). A fixed-ring Consolidometer, but the base was sealed was also used to measure the pore pressure with a transducer (Smith and Wahls, 1969). A general-purpose Consolidometer for CRS tests in which the specimen is saturated at a constant volume under a back pressure with no lateral strain was also proposed (Wissa et al., 1971). The triaxial cell was modified to include a consolidation ring and loading press to deform the specimen at a constant rate (Gorman et al., 1978). The CRS apparatus was modified to measure the permeability and pore pressure at the base (Armour and Drnevich, 1986). The triaxial cell was further modified by placing the consolidation ring within and connecting the base to the outlet port (Vikash, 2013). ASTM D4186-12 (2012) calls for a standard apparatus similar to that developed by Wissa et al. (1971). A simple CRS test apparatus like an oedometer cell is lacking in the literature. Figure 1 presents a vertical cross-section of the CRS test apparatus developed by Wissa et al.

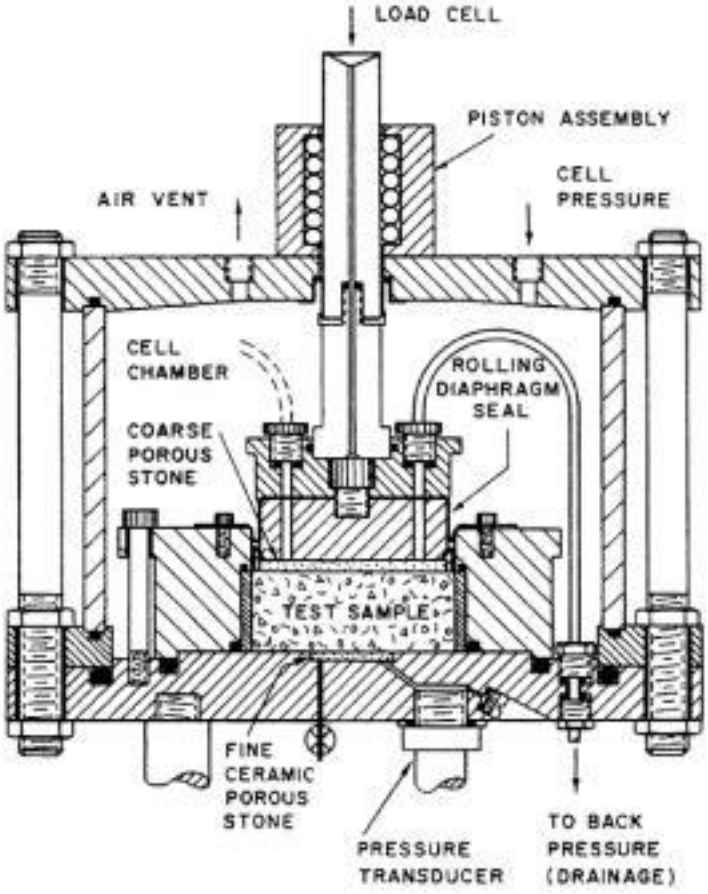

Fig. 1: MIT general-purpose Consolidometer (Wissa et al. 1971).

3.2.2. Theoretical Background

Smith and Wahls (1969) were the first to develop a theory and approximate solution for the CRS consolidation test. They showed that the void ratio varies according to depth and time. However, their theory has two major issues: the assumption that the void ratio is a linear function of time and depth is difficult to evaluate, and they assumed an unknown

parameter b with no procedure for determining it. A reference test on similar specimens is needed because the results depend on b. Wissa et al. (1971) ignored some of Smith and Wahls's (1969) assumptions in developing a more comprehensive theory based on strain distribution across the specimen's depth, which they used to formulate the governing equation and derive transient and steady-state solutions. Since then, Wissa et al.'s (1971) theory has been widely used to interpret CRS test data by incorporating it into ASTM D4186-82 (1982). Yoshikuni et al. (1995) developed a simpler theory based on the assumption that the strain rate at every location is equal to the average strain once a steady state is reached. Smith and Wahls (1969) did not consider the transient state. Thus, the theories of Wissa et al. (1971) and Yoshikuni et al. (1995) are better for analyzing CRS test data because the transient state is likely to occur.

Few theories are available for interpreting the consolidation test results under a large strain. Umehara and Zen (1980) and Lee (1981) developed theories and numerically solved the governing differential equations using appropriate boundary conditions and assuming non-dimensional parameters. They used charts to set the consolidation parameters. However, no rational method has been reported for choosing the curve that best approximates material behavior. Vikash (2013) developed a moving boundary theory.

To obtain compressibility results that match the measurements of an oedometer, an appropriate strain rate must be selected for the CRS test. Smith and Wahls (1969) performed CRS tests on Massena clay and calcium montmorillonite and compared the results with conventional measurements. They found that the curves representing the relationship between the void ratio e and the logarithm of the effective stress σ'v for the CRS tests differed from those of the conventional measurements at higher strain rates. A high strain rate rapidly increases the excess pore pressure, which causes the pre-consolidation pressure to be overestimated and prevents the steady-state condition. A low strain rate results in no significant increase in the pore water pressure, which causes the coefficient of consolidation cv to be unreasonably high (Smith and Wahls, 1969). Several researchers have suggested guidelines for selecting an appropriate strain rate for CRS tests. Smith and Wahls (1969) proposed a theoretical model where the consolidation parameters are in the strain equation.

Before the CRS test, some parameters must be assumed. Lee (1981) proposed a dimensionless strain parameter based on cv. Armour and Drnevich (1986) calculated the strain rate based on the liquidity index and permeability. ASTM D4186-82 (1982) recommends using the liquid limit as the basis. However, the soil classification was revised in 2012. The available methods require critical parameters or empirical relations. Fixing the strain rate according to the liquid limit is problematic because cv may differ for two soils with the same liquid limit. Furthermore, soil in the same group can have different cv values. Crawford (1988) reported that the strain rate does not depend on the liquid limit. In addition, the maximum allowable pore pressure ratio ru (i.e., the ratio of pore pressure developed at the base of the specimen to the applied total stress) ranges from 3% to 50%, depending on the researcher. ASTM D4186-12 (2012) recommends a pore pressure ratio range of 3%–15%, which is commonly used.

$$\delta_c = 0.0001 \, . \sigma_c \tag{1}$$

Where, δ_c is the deflection due to variations in cell pressure (cm) and σ_c is the cell pressure (kg/cm^2).

3.2.3. Data Analysis

The CRS test data can be used to quickly estimate engineering properties, in contrast to the time-consuming process needed to interpret oedometer measurements. The equations utilized for data interpretation are as follows:

$$\sigma_{n,v} = \left(\frac{P_{n,L} - P_c}{A_L}\right) \tag{2}$$

Where, $\sigma_{n,v}$ is the axial stress applied to the specimen at any moment (kg/cm2); $P_{n,L}$ is the axial force applied to the loading piston at any moment (kg); P_c is the correction of the axial force to account for the external force induced by the back pressure on the sealing and piston unit; and A_L is the cross-sectional area of the specimen during loading (cm^2).

3.3 Strain Equations

3.3.1 Linear Theory

Wissa et al. (1971) proposed the strain equation based on the linear theory, where c and kg are measured and a is solved. The vertical effective stress is denoted as σ_v' , and Δu_b is measured for a provided period at discrete points:

$$\sigma_v' = \sigma_v - \frac{2}{3} . \Delta u_b \quad (3)$$

Where, σ_v is the total vertical stress at a given time; Δu_b is the excess pore water pressure of the specimen at the given time.

3.3.2 Nonlinear Theory

The nonlinear theory evaluates variables to measure cv and k. a is utilized to evaluate k with at discrete measurement points:

$$\sigma_v' = (\sigma_v^3 - 2.\sigma_v^2 . \Delta u_b + \sigma_v . \Delta u_b^2)^{1/3} \quad (4)$$

Where, σ_v' is the average effective stress of a specimen at a given time and Δu_b is the excess pore-water pressure at the specimen base for a given time. The coefficient of consolidation cv is obtained by:

$$c_v = -\frac{H^2.log\left[\frac{\sigma_{v2}}{\sigma_{v1}}\right]}{2.\Delta t.log\left[1-\frac{\Delta u_b}{\sigma_v}\right]} \quad (5)$$

Rearranging Equation (5) obtains the hydraulic conductivity k:

$$k = c_v.m_v.\gamma_w \quad (6)$$

Where, m_v is the coefficient of volumetric compressibility and γ_w is the unit weight of water.

$$m_v = \frac{0.434 .r.\Delta t}{\sigma_v' .log\left[\frac{\sigma_2}{\sigma_1}\right]} \quad (7)$$

Substituting Equations (5) and (7) into Equation (6) obtains:

$$k = -\frac{0.434 .r .H^2.\gamma_w.\Delta t}{2.\sigma_v' .log\left[1-\frac{\Delta u_b}{\sigma_v}\right]} \quad (8)$$

When $\Delta u_b / \sigma_v$ (i.e., the ratio of the excess pore pressure u_b in the undrained face to the total vertical stress σ_v) is small, the expressions obtained from different stress–strain relationships are very similar, and they begin to diverge as $\Delta ub/\sigma v$ increases. For more information, see Wissa et al. (1971).

4. Results and Discussion

Experimental tests were performed on RBBC, RVS, and VBC samples, and the results were compared with prior results. Table 2 summarizes consolidation test results based on the conventional 1D oedometer and CRS Rowe cell tests for RBBC. Tables 3 and 4 define the index properties of RBBC, including the specific gravity (Gs), liquid limit (W_L), plastic limit (W_P), and plasticity index (I_P).

Table 2: Summary of consolidation test results.

Test Number	Vertical Strain Rate $\varepsilon_{v\ (\%\ /\ hr.)}$	Initial Specimen Height H_o (mm)	Initial Water Content w_o (%)	Initial Void Ratio e_o	σ'_p (kPa)	σ'_{vm} (kPa)	CR	Maximum $\Delta u_b / u_b$ (%)
a. Test type: 1D Incremental Loading Oedometer ***(63.5*** mm Diameter Specimen)								
1	IL	22.86	45.26	1.227	100	-	0.175	-
2	IL	22.86	46.36	1.246	91	-	0.169	-
3	IL	22.86	45.96	1.280	92	-	0.175	-
4	IL	22.86	46.78	1.271	95	-	0.174	-
b. Test Type: 1D Constant Rate of Strain (CRS): Rowe Cell ***(151*** mm Diameter Specimen)								
5	0.12	59.2	45.26	1.281	103	340	0.159	2.2
6	0.09	59.9	46.32	1.279	93	321	0.150	3.4
7	0.10	61.8	44.13	1.236	95	349	0.160	1.0
8	1.00	63.6	47.26	1.305	96	367	0.153	21.8
9	1.00	62.8	47.86	1.337	88	346	0.157	17.8
10	1.00	61.8	47.64	1.339	89	329	0.157	18.6
11	3.00	55.2	47.37	1.225	97	442	0.165	67.8
12	3.00	63.8	47.37	1.320	96	510	0.160	77.0
13	3.00	64.8	44.13	1.338	93	420	0.152	70.9

Where IL = incrementally loaded

Table 3: Index properties of RBBC from Series IV (after Cauble 1996).

Year	**Researcher**	**Source Batch**	G_s	W_L	W_P	I_P	**Clay < 2 µm (%)**	**Organic Content**	**Salt (g/L)**
1994	**Zriek**	**powder**	**2.78**						
1994	**Sinfield**	**402** **403**							
1996	**Cauble**	**Powder** **401** **404** **405** **406** **407** **408** **409** **410** **411** **413** **414** **415** **416** **417**	**2.81**	 **46.7** **47.4** **45.2** **45.0** **44.6** **44.7** **45.4** **46.6** **46.7** **45.5** **46.3** **46.1** **46.7** **47.2**	 **46.7** **47.4** **45.2** **45.0** **44.6** **44.7** **45.4** **46.6** **46.7** **45.5** **46.3** **46.1** **46.7** **47.2**	 **21.8** **21.9** **22.1** **22.6** **23.0** **23.9** **24.0** **25.0** **24.5** **24.3** **24.3** **24.7** **24.0** **24.5**	 **24.9** **25.5** **23.1** **22.4** **21.6** **20.8** **21.4** **21.6** **22.2** **21.2** **22.0** **21.4** **22.7** **22.7**	 **57.6** **57.8** **58.7** **56.8** **56.9**	 **10.4** **10** **12.5** **13.1** **10.1** **13** **13.4** **10.2** **9.7** **12** **10.5** **12.9** **13.2**
1998	**Santagata**	**418** **419**		**47.8**	**23.3**	**24.5**			
1998	**Current research**	**420**		**45.2**	**22.6**	**22.6**			
	Average	**Powder** **401 - 411** **413 - 420**	**2.80**	**46.2** **±0.9**	**23.4** **±1.1**	**22.8** **±1.4**	**58.0** **±1.2**	**4.4**	**11.6** **±1.5**

Table 4: Index properties of RBBC samples from Series I–III (after Cauble 1996).

Year	**Researcher**	**Source Batch**	G_s	W_L	W_P	I_P	Clay < 2µm (%)	Salt (g/L)
1961	Bailey	MIT-1139	2.77	30.0 34.7	17.5 17.7	12.5 17.0	40	2-3 35
1963	Jackson			36.2	19.5	16.7		16.7
1964	Varallyay	S4 SS S6		32.6 33.3 32.8	19.5 20.4 20.3	13.1 12.9 12.5	35	16.8 16
1965	Ladd, R.S.		2.77	45.0	22.0	23.0		I6
1965	Preston	SI	2.77	45.6	23.4	22.2	35	24
1966	Braathen	S2	2.77	45.4	23.l	22.3		22
1967	Dickey			34.5	23.9	19.6		

1970	Kinner	1OO 150 200 300 400 800 900 1000 1100 1200 M101 M104 M107 M200 M400	2.78	43.5 43.5 38.1 39.7 39.4 41.5 41.2 41.1 42.0 40.2 40.7 40.3 41.3 42.3 39.8	19.6 19.6 17.8 21.6 21.3 19.5 18.7 19.5 20.6 18.6 19.6 19.6 19.6 18.5 18.9	23.9 23.9 20.3 18.1 18.1 22.0 22.5 22.6 21.4 21.6 21.1 20.7 21.7 23.8 20.9	50 52 52 48 54 58 48 52 52 47	 8 10 10 16 16 16 16 I6
1971	Ladd et al.	160 1300 1500	2.78	38.I 42.I 43.8	I7.8 22.1 20.6	20.3 20.0 23.2		8 16 16
1984	Bensari	105 111	2.75 2.75	47.6 47.l	23.3 24.9	24.3 22.2		I6 16
1985	O'Neill	105-112	2.78	41.3	22.1	19.2	52	16
1989	Seah	200-207	2.78	45.2	21.7	23.5	58	16
1991	Sheahan	210,214, 216		45.6	21.4	24.2		
1993	Cauble	217-218	2.78	37.0	21.3	15.7		
1994	Santagata	219-220		40.4	20.9	19.5		

Figure 2 shows the grain-size distribution (GSD) curves for five different batches starting from Series IV before the sedimentation process. The data were consistent with an average clay fraction of 58±1.2%. The salt content was calculated by measuring the conductivity and scaling it against the KCL standard. The average salt content was 11.6±1.5 g/L. The salt content was modified in batches to obtain a concentration of 16 g/L, which helped manage the clay fabric. However, the recent batches were not properly modified, which resulted in a lower value. Only RVBC 101 was classified as CH, whereas the other soils were classified as CL. Figure 3 shows the GSDs for the RVBC and RVS samples. The plots utilize the USCS classification system with an approximate clay fraction of 47%.

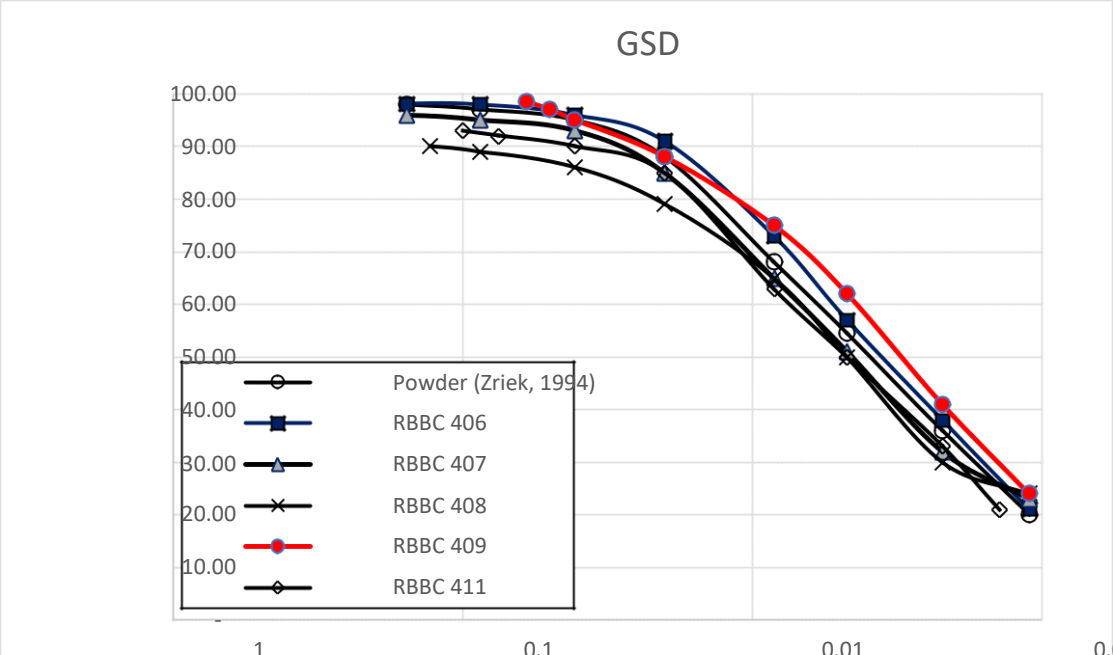

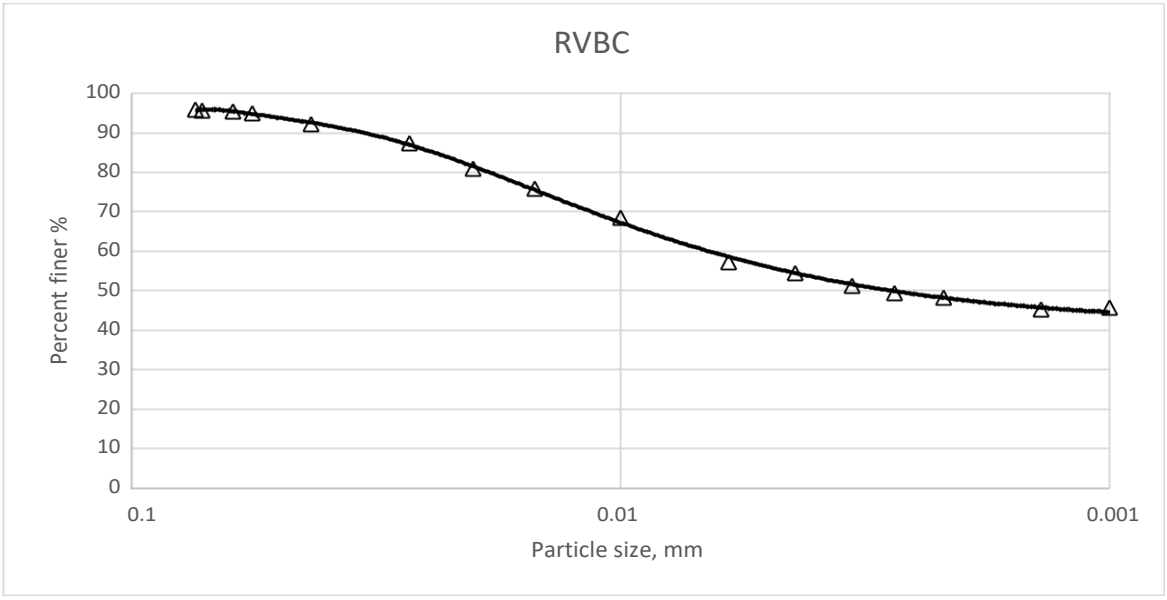

(a)

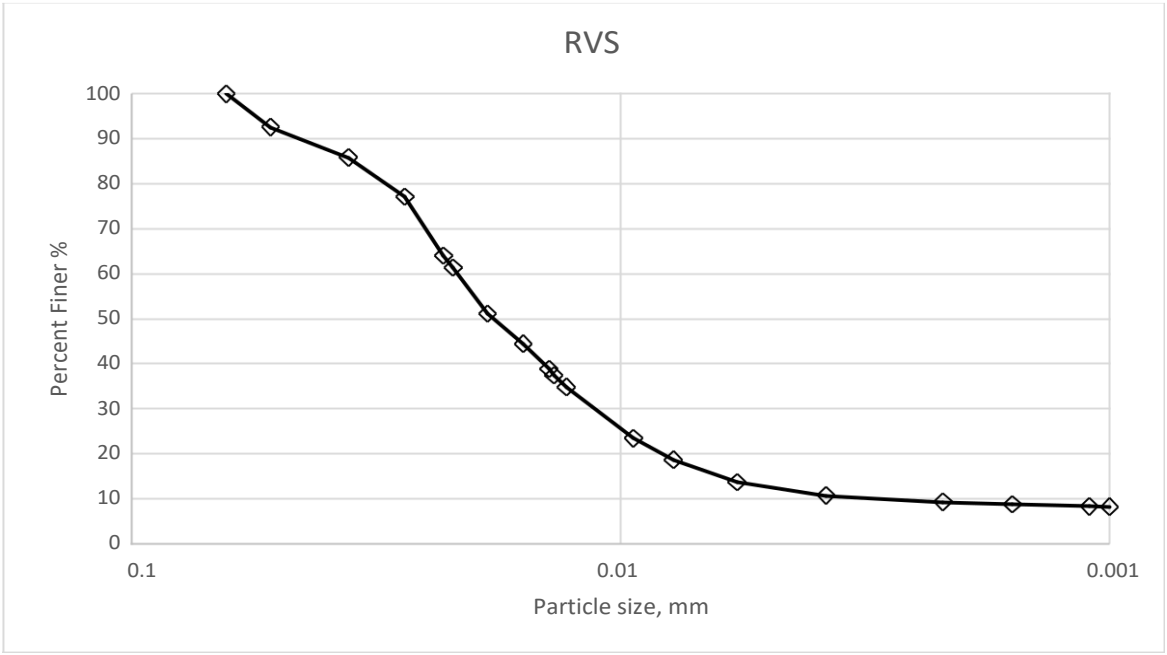

(b)

Fig. 3: Grain size distributions of (a) RVBC and (b) RVS.

Table 5 summarizes the results of 23 CRS tests performed on RVBC, RVS, and RBBC samples using Wissa's consolidometer.

Table 5: CRS test results for RVBC, RVS, and RBBC samples using Wissa's consolidometer.

Test No.	H_o (cm)	ε_{rate} (%) / (hr.)	cell pressure U_b (kg /cm^2)	w_o (%)	S_o (%)	γ_{bo} (g / cm^3)	e_o	Compression Results		Coefficient of Consolidation	Hydraulic conductivity
								Cc	e	C_v (cm^2 / sec)	K (cm/sec)
1	2.35	1.58	3.92	41.1	99.7	1.804	1.12	0.408	0.98	4.37E-04	2.51E-08
2	2.35	1.56	3.88	41.2	99.6	1.802	1.122	0.409	0.984	4.16E-04	2.29E-08
3	2.35	0.85	3.91	40.6	99.8	1.812	1.102	0.425	0.976	3.23E-04	2.27E-08
4	2.35	0.85	3.94	40.2	99.1	1.807	1.101	0.423	0.966	3.65E-04	2.86E-08
5	2.36	0.55	3.91	38.8	97.6	1.808	1.079	0.426	0.96	3.38E-04	2.96E-08
6	2.35	0.15	3.94	39.6	98.7	1.812	1.088	0.421	0.977	3.23E-04	2.38E-08
7	2.34	3.88	3.94	39	98.6	1.816	1.073	0.368	0.987	8.50E-04	3.40E-08
8	2.35	0.15	3.9	39.7	98.8	1.813	1.09	0.426	0.971	3.74E-04	3.08E-08
9	2.35	3.93	3.95	40.4	99.3	1.807	1.105	0.369	1.015	8.50E-04	2.33E-08
10	2.35	0.55	3.95	40.7	99.6	1.808	1.107	0.434	0.963	3.23E-04	3.08E-08
11	2.36	0.84	3.92	44.3	100.5	1.794	1.212	0.36	1.073	2.40E-03	1.04E-07
12	2.35	0.85	3.95	44.4	110.7	1.973	1.213	0.364	1.07	2.40E-03	1.10E-07
13	2.34	1.35	3.9	44.2	100.9	1.799	1.205	0.373	1.072	2.40E-03	1.14E-07
14	2.35	12.71	3.91	44	100.9	1.801	1.199	0.376	1.084	3.00E-03	1.03E-07
15	2.35	4.02	4.02	44.3	101.3	1.801	1.201	0.387	1.084	2.60E-03	1.20E-07
16	2.36	0.15	3.89	44.2	100.4	1.794	1.212	0.36	1.07	2.56E-03	1.09E-07
17	2.35	0.07	3.87	44.2	101.4	1.804	1.20	0.369	1.066	2.58E-03	1.10E-07
18	2.36	3.04	3.27	43.6	100.6	1.807	1.204	0.363	1.098	2.30E-03	9.28E-08
19	2.35	48.1	3.99	43.9	101.9	1.816	1.199	0.362	1.118	8.00E-03	1.00E-07
20	2.35	74.1	3.92	43.9	102.4	1.821	1.192	0.362	1.131	3.50E-03	1.03E-07
21	2.32	7.83	9.97	42.6	101.3	1.825	1.169	0.361	1.079	2.60E-03	1.12E-07
22	2.35	7.79	3.95	42.5	100.8	1.821	1.171	0.361	1.091	2.60E-03	1.05E-07
23	2.34	3.76	3.96	42.1	100.9	1.826	1.161	0.365	1.077	2.30E-03	1.05E-07

5. Conclusions

This study summarized the results of CRS tests on RBBC and RVBC samples. The CRS tests utilized a Wissa Consolidometer at various strain rates of 0.155%/h–3.96%/h for the RVBC samples and 0.07%/h–74.10%/h. Numerical experimental analyses were performed based on the CRS equations and test results. General trends were obtained for effects of the strain rate on the CRS test results. Future work will involve improving the soil model to estimate the effects nonlinear and linear theories, which may add insights for further interpretation of CRS test data.

Data Availability

The datasets generated during and/or analysed during the current study are available from the corresponding author on reasonable request.

Conflicts of Interest

The author declares that he has no conflicts of interest.

Funding Statement

The author received no financial support for the research, authorship, and/or publication of this article.

Acknowledgments

The authors would like to thank Enago (www.enago.com) for the English language review.

References

[1] Adajar, M.A.Q. and Cutora, M.D., 2018. The effect of void ratio, moisture content and vertical pressure on the hydrocompression settlement of copper mine tailing. GEOMATE Journal, 14(44), pp.82-89.

[2] Akbarimehr, D. and Aflaki, E., 2019. Using empirical correlations to evaluate the compression index of Tehran clay. AUT Journal of Civil Engineering, 3(1), pp.129-136.

[3] Alam, M., Shahriar, A.R., Islam, M.S., Islam, N. and Abedin, M., 2021. Experimental investigation on the strength and deformation aspects of thixotropic aging in reconstituted clays. Geotechnical and Geological Engineering, 39(3), pp.2471-2486.

[4] Al-Taie, A.J., Al-Bayati, A.F. and Taki Z.N.M., 2017. Compression index and compression ratio prediction by artificial neural networks. Journal of Engineering, 23(12), pp.96-106.

[5] Amrani, M., Taha, Y., Elghali, A., Benzaazoua, M., Kchikach, A. and Hakkou, R., 2021. An experimental investigation on collapsible behavior of dry compacted phosphate mine waste rock in road embankment. Transportation Geotechnics, 26, p.100439.

[6] Bag, R. and Rabbani, A., 2017. Effect of temperature on swelling pressure and compressibility characteristics of soil. Applied Clay Science, 136, pp.1-7.

[7] Chen, R., Xu, T., Lei, W., Zhao, Y. and Qiao, J., 2018. Impact of multiple drying–wetting cycles on shear behaviour of an unsaturated compacted clay. Environmental Earth Sciences, 77(19), pp.1-9.

[8] Chhun, K.T., Lee, S.H., Choi, Y.T. and Yune, C.Y., 2018, June. Experimental Study on the Effect of Compaction on Long- term Settlement of the Embankment of High-speed Railways. In The 28th International Ocean and Polar Engineering Conference. OnePetro.

[9] Dagdeviren, U., Demir, A.S. and Kurnaz, T.F., 2018. Evaluation of the compressibility parameters of soils using soft computing methods. Soil Mechanics and Foundation Engineering, 55, pp.173-180.

[10] Fikret Kurnaz, T., & Kaya, Y. (2018). The comparison of the performance of ELM, BRNN, and SVM methods for the prediction of compression index of clays. Arabian Journal of Geosciences, 11(24), 1-14.

[11] Girgis, N., Li, B., Akhtar, S. and Courcelles, B., 2020. Experimental study of rate-dependent uniaxial compressive behaviors of two artificial frozen sandy clay soils. Cold Regions Science and Technology, 180, p.103166.

[12] Habibbeygi, F., 2017. Determination of the compression index of reconstituted clays using intrinsic concept and normalized void ratio. International Journal of Geomate, 13, pp.54-60.

[13] Habibbeygi, F. and Nikraz, H., 2018. The effect of unloading and reloading on the compression behaviour of reconstituted clays. GEOMATE Journal, 15(51), pp.53-59.
[14] Hamilton, J.J. and Crawford, C.B., 1960. Improved determination of preconsolidation pressure of a sensitive clay. Special Technical Publication, 254, pp.254-270.
[15] Howald, E.P. and Torche, J., 2020. Global Warming and Loss of Bearing Capacity of Permafrost: An Experimental Study on the Effects of Freezing/Thawing Cycles on a Silty Soil. Global Journal of Earth Science and Engineering, 7, pp.1-21.
[16] Kaddouri, Z., Cuisinier, O. and Masrouri, F., 2019. Influence of effective stress and temperature on the creep behavior of a saturated compacted clayey soil. Geomechanics for Energy and the Environment, 17, pp.106-114.
[17] Krim, A., Arab, A., Chemam, M., Brahim, A., Sadek, M. and Shahrour, I., 2019. Experimental study on the liquefaction resistance of sand–clay mixtures: Effect of clay content and grading characteristics. Marine Georesources & Geotechnology, 37(2), pp.129-141.
[18] Kumar, R., Jain, P.K. and Dwivedi, P., 2016. Prediction of compression index (Cc) of fine grained remolded soils from basic soil properties. International Journal of Applied Engineering Research, 11(1), pp.592-598.
[19] Kurnaz, T.F., Dagdeviren, U., Yildiz, M. and Ozkan, O., 2016. Prediction of compressibility parameters of the soils using artificial neural network. Springerplus, 5, pp.1801.
[20] Li, M., Cong, X., Zhu, L., Kong, L., Zhang, Z., Tian, A. and Li, L., 2017. Experimental study on recycling dredged marine sediment and phosphate tailing to produce earth fill. Marine Georesources & Geotechnology, 35(4), pp.586-591.
[21] Liu, Z., Liu, J., Li, X. and Fang, J., 2019. Experimental study on the volume and strength change of an unsaturated silty clay upon freezing. Cold Regions Science and Technology, 157, pp.1-12.
[22] Mohammadzadeh, S.D., Bolouri, B.J., Vafaee, J.Y.S.H. and Alavi, A.H., 2016. Deriving an intelligent model for soil compression index utilizing multi-gene genetic programming. Environmental Earth Sciences, 75, pp.262.
[23] Mohammadzadeh S, D., Kazemi, S. F., Mosavi, A., Nasseralshariati, E., & Tah, J. H. (2019). Prediction of compression index of fine-grained soils using a gene expression programming model. Infrastructures, 4(2), 26.
[24] MolaAbasi, H., Shooshpasha, I. and Ebrahimi A., 2016. Prediction of compression index of saturated clays (Cc) using polynomial models. Scientica Iranica, 23(2), pp.500-507.
[35] Nesamatha, R. and Arumairaj, P.D, 2015. Numerical modeling for prediction of compression index from soil index properties. Electronic Journal of Geotechnical Engineering, 20, pp.4369-4378.
[25] Onyelowe, K.C., Ebid, A.M., Nwobia, L. and Dao-Phuc, L., 2021. Prediction and performance analysis of compression index of multiple-binder-treated soil by genetic programming approach. Nanotechnology for Environmental Engineering, 6(2), pp.1-17.
[26] Pandya, S. and Sachan, A., 2019. Experimental studies on effect of load repetition on dynamic characteristics of saturated Ahmedabad cohesive soil. International Journal of Civil Engineering, 17(6), pp.781-792.
[27] Pestana, J.M. and Whittle, A.J., 1999. Formulation of a unified constitutive model for clays and sands. International Journal for Numerical and Analytical Methods in Geomechanics, 23(12), pp.1215-1243.
[28] Polidori, E., 2015. On the intrinsic compressibility of common clayey soils. European Journal of Environmental and Civil Engineering, 19(1), pp.27-47.
[29] Shahriar, A.R. and Jadid, R., 2018. An experimental investigation on the effect of thixotropic aging on primary and secondary compression of reconstituted dredged clays. Applied Clay Science, 162, pp.524-533.
[30] Smith, R.E. and Wahls, H.E., 1969. Consolidation under constant rate of strain. Journal of the Soil Mechanics and Foundations Division, 95(2), pp.519- 539.
[31] Soni, A. and Varshney, D., 2021, April. Experimental study of the effect of alkali contamination on geo-mechanical properties of the soil. In IOP Conference Series: Materials Science and Engineering (Vol. 1116, No. 1, p. 012173). IOP Publishing.
[32] Wang, Y., Li, X. and Zheng, B., 2018. Experimental study on mechanical properties of clay soil under compression by ultrasonic test. European Journal of Environmental and Civil Engineering, 22(6), pp.666-685.
[33] Wen, T., Wang, P., Shao, L. and Guo, X., 2021. Experimental investigations of soil shrinkage characteristics and their effects on the soil water characteristic curve. Engineering Geology, 284, p.106035.

[34] Wickrama Kaluthota Hewage, R.E.W., 2018. An experimental study on time-dependent behaviour of reconstituted clayey soils in 1D and triaxial compression.
[35] Wissa, A.E.Z., Christian, J.T., Davis, E.H. and Heiberg, S., 1971. Consolidation at constant rate of strain. Journal of the Soil Mechanics and Foundations Division, 97(10), pp.1393-1413.